analytical chemistry

Subscriber access provided by SEOUL NATL UNIV

Article

Construction and Performance Test of a Multiplexed Multistage (MS) Time-of-Flight Mass Spectrometer

Young Sik Shin, Jeong Hee Moon, and Myung Soo Kim

Anal. Chem., **2008**, 80 (24), 9700-9704 • Publication Date (Web): 12 November 2008

Downloaded from http://pubs.acs.org on December 15, 2008

More About This Article

Additional resources and features associated with this article are available within the HTML version:

- Supporting Information
- Access to high resolution figures
- Links to articles and content related to this article
- Copyright permission to reproduce figures and/or text from this article

View the Full Text HTML

ACS Publications
High quality. High impact.

Analytical Chemistry is published by the American Chemical Society. 1155 Sixteenth Street N.W., Washington, DC 20036

Anal. Chem. **2008,** *80,* 9700–9704

Construction and Performance Test of a Multiplexed Multistage (MS^n) Time-of-Flight Mass Spectrometer

Young Sik Shin,[†] Jeong Hee Moon,[‡] and Myung Soo Kim*,[†]

Department of Chemistry, Seoul National University, Seoul 151-742, Korea, and Systemic Proteomics Research Center, KRIBB, Daejeon 305-806, Korea

A time-of-flight mass spectrometer equipped with two reflectrons was constructed for multiplexed photodissociation tandem mass spectrometry of peptide ions generated by matrix-assisted laser desorption ionization. A linear reflectron was used for high-resolution selection of a precursor ion while a quadratic reflectron was used for product ion analysis. With the photoexcitation of a precursor ion inside a cell floated at high voltage, information (MS^3) on intermediate ions generating a particular product ion was obtained. Fully multiplexed detection resulted in good MS^3 signal levels. Use of the quadratic reflectron allowed intermediate ion mass determination within 4 Da. The possibility of further extending the technique and its analytical potential are discussed.

Tandem mass spectrometry[1−4] is a useful technique for the structural and mechanistic studies on polyatomic ions. In two-stage tandem mass spectrometry (MS/MS or MS^2), a precursor ion is selected by the first-stage mass analyzer and its dissociation product ions are analyzed by the second-stage analyzer. Collision with a neutral gas (collisionally activated dissociation, CAD[4,5]) and photoexcitation (photodissociation, PD[6,7]) are popular techniques for ion activation. A similar tactic, viz., precursor ion selection and activation followed by product ion analysis, can be used to get information on a product ion formed in MS^2, resulting in MS^3.

In tandem mass spectrometers utilizing trapping-type analyzers,[8,9] one and the same analyzer can handle multiple stages of tandem mass spectrometry. In contrast, for instruments utilizing spatially separated analyzers,[10,11] the number of analyzers must be increased as n in MS^n increases, resulting in complicated and expensive instruments. A common problem in MS^n is that signal intensities decrease rapidly as n increases. Fourier transform-mass spectrometry[8] (FT-MS) is more advantageous than others because of its inherent capability of simultaneous (multiplexed) and repeated detection. FT-MS is especially useful for MS^3 of biological molecules[12] because ion signal levels from these molecules generated by common ionization techniques such as electrospray ionization and matrix-assisted laser desorption ionization (MALDI) are very low. Even though the time-of-flight (TOF) analyzer is also capable of multiplexed detection, sequential operation in the form of TOF−TOF[13,14] has been the usual scheme of its use. Sequential MS^n beyond MS^2 for MALDI-TOF is probably impractical because of the extremely low signal levels expected.

As a part of our effort to optimize MALDI-tandem TOF utilizing UV-PD,[15−17] we attempted to estimate the time scale of PD by photoexciting a precursor ion (m_1^+) inside a cell floated at high voltage.[18] We hoped to observe splitting of each product ion (m_2^+) peak into two components, one due to its formation inside the cell (in-cell component, formed within 100 ns) and the other outside the cell (postcell component, formed on the 100 ns to 10 μs time scale). Surprisingly, additional components lying between the two components were observed. Detailed analysis showed that these were due to formation of m_2^+ from m_1^+ through consecutive reactions via various intermediate ions (m_i^+), viz., $m_1^+ \rightarrow m_i^+ \rightarrow m_2^+$ with the first step occurring inside the cell and the second step outside. Recording the PD spectrum of m_1^+ without the cell voltage, viz., collection of m_2^+, corresponds to usual tandem mass spectrometry or MS^2. In contrast, collecting m_i^+ data for each m_2^+ with the cell voltage on corresponds to MS^3, viz., a "constant

* To whom correspondence should be addressed. Prof. Kim, Department of Chemistry, Seoul National University, Seoul 151-742, Korea. E-mail: myungsoo@snu.ac.kr.

[†] Seoul National University.

[‡] Systemic Proteomics Research Center, KRIBB.

(1) Busch, K. L.; Glish, G. L.; McLuckey, S. A. *Mass Spectrometry/Mass Spectrometry*; VCH: New York, 1988.
(2) Kinter, M.; Sherman, N. E. *Protein Sequencing and Identification Using Tandem Mass Spectrometry*; John Wiley: New York, 2000.
(3) Hernandez, P.; Muller, M.; Appel, R. D. *Mass Spectrom. Rev.* **2006**, *25*, 235–254.
(4) McLafferty, F. W. *Tandem Mass Spectrometry*; Wiley-Interscience: New York, 1983.
(5) Cooks, R. G. In *Collision Spectroscopy*; Plenum: New York, 1978.
(6) Park, S. T.; Kim, S. K.; Kim, M. S. *Nature* **2002**, *415*, 306–308.
(7) Dunbar, R. C.; Bowers, M. T. *Gas Phase Ion Chemistry*; Academic Press: New York, 1984.
(8) Marshall, A. G.; Hendrickson, C. L.; Jackson, G. S. *Mass Spectrom. Rev.* **1998**, *17*, 1–35.
(9) Jonscher, K. R.; Yates, J. R. *Anal. Biochem.* **1997**, *244*, 1–15.
(10) Mann, M.; Hendrickson, R. C.; Pandey, A. *Annu. Rev. Biochem.* **2001**, *70*, 437–473.
(11) Biemann, K.; Martin, S. A. *Mass Spectrom. Rev.* **1987**, *6*, 1–75.
(12) Solouki, T.; Paša-Tolić, L.; Jackson, G. S.; Guan, S. G.; Marshall, A. G. *Anal. Chem.* **1996**, *68*, 3718–3725.
(13) Medzihradszky, K. F.; Campbell, J. M.; Baldwin, M. A.; Falick, A. M.; Juhasz, P.; Vestal, M. L.; Burlingame, A. L. *Anal. Chem.* **2000**, *72*, 552–558.
(14) Mirsaleh-Kohan, N.; Robertson, W. D.; Compton, R. N. *Mass Spectrom. Rev.* **2008**, *27*, 237–285.
(15) Oh, J. Y.; Moon, J. H.; Kim, M. S. *J. Am. Soc. Mass Spectrom.* **2004**, *15*, 1248–1259.
(16) Yoon, S. H.; Moon, J. H.; Choi, K. M.; Kim, M. S. *Rapid Commun. Mass Spectrom.* **2006**, *20*, 2201–2208.
(17) Moon, J. H.; Shin, Y. S.; Cha, H. J.; Kim, M. S. *Rapid Commun. Mass Spectrom.* **2007**, *21*, 359–368.
(18) Yoon, S. H.; Kim, M. S. *J. Am. Soc. Mass Spectrom.* **2007**, *18*, 1729–1739.

10.1021/ac801675r CCC: $40.75 © 2008 American Chemical Society
Published on Web 11/12/2008

granddaughter ion" spectrum. Unlike in conventional MS^3, only one activation step was used here. Simultaneous, or multiplexed, detection for all m_2^+ resulted in good signal levels for MS^3.

PD inside the voltage-floated cell resembles the retarding/accelerating field technique for MS^2 used with early TOF spectrometers.[19,20] In modern tandem TOF spectrometers equipped with a reflectron with linear potential inside, or linear reflectron, a voltage-floated collision cell is used for the high resolution detection of CAD product ions (MS^2). Such voltage lifting is not needed when a nonlinear reflectron such as the curved-field reflectron reported by Cornish and Cotter[21] is used. More advanced MS^2 TOF designs utilizing two reflectrons were also reported. In all the cases, a linear reflectron was used for high-resolution selection of a precursor ion. A curved-field[21,22] or quadratic[23] reflectron was used as the MS^2 analyzer. The instrument designed by Enke et al.[22] was used for PD at the MS^2 level.

Reliable mass calibration for m_i^+ was difficult in our cell PD work due to partial compensation for the flight time spread of m_2^+ by the linear potential component of the reflectron used in the study. To handle this problem, we have built a new instrument using a quadratic reflectron. Other improvements over the previous apparatus include the installation of a linear reflectron for temporally stable selection of a precursor ion. Design of the new instrument and its overall performance are reported in this paper.

EXPERIMENTAL SECTION

Instrument Design. SIMION[24] calculation was utilized to design the PD-tandem TOF mass spectrometer built in this work. A schematic drawing of the instrument is shown in Figure 1. The apparatus consists of a MALDI source with delayed extraction (18 kV dc plus 1.58 kV ac), a linear reflectron (23.28 kV), a voltage-floated PD cell, a quadratic reflectron (or "perfectron"[25]), and the final detector (MCP, 40 mm o.d., Burle, Lancaster, PA). The distance between the MALDI source exit and the linear reflectron entrance is 1250 mm. Two ion gates are installed on the ion trajectory, one at 70 mm in front of and the other at 52 mm after the reflectron. A stainless steel tube (20 mm o.d. and 500 mm length) is installed between the MALDI source and the linear reflectron to shield ion beams from the stray field. To guide the precursor ion beam, two deflectors are installed at 103 mm, one in front of and the other after the reflectron.

The linear reflectron has a 210 mm length, and its time image (the second time focus) is at 370 mm from the exit. As in the TOF instruments equipped with two reflectrons reported previously,[21−23] this reflectron is simply for high-resolution selection of a precursor ion, viz., it is not the second-stage analyzer for tandem mass spectrometry.

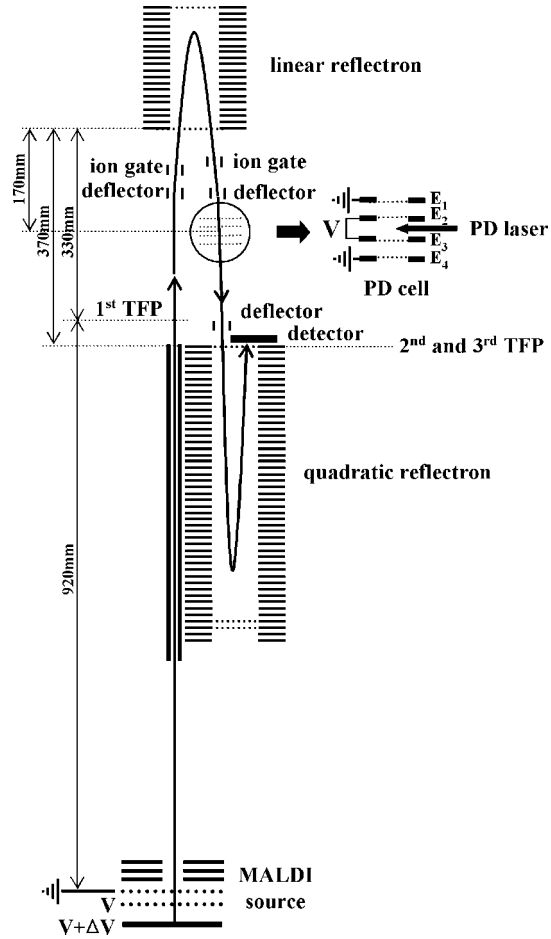

Figure 1. A schematic of the PD tandem TOF built in this work. Time-focusing planes are marked as TFPs. A temporally stable "A" peak pulse of a precursor ion is selected by the linear reflectron and is synchronized with a PD laser pulse at the center the voltage-floated PD cell. The PD cell consists of four electrodes. Product ions formed inside and outside the cell and those formed via consecutive reactions are analyzed by the quadratic reflectron.

The center of the PD cell assembly consisting of four apertures, E1−E4, is at 170 mm from the linear reflectron exit. E1 and E4 are grounded, and E2 and E3 are at the same voltage. E1−E2, E2−E3, and E3−E4 distances are 9.5, 11.5, and 9.5 mm, respectively. The PD laser passes between E2 and E3. Grids with 95% transmission are mounted on E1, E2, and E4. On E3, the 90% grid is mounted to suppress transmission of ions generated from residual gas by the PD laser. Deflection of the ion beam for optimum reflection in the quadratic reflectron necessitates slight tilting (around 3°) of the PD cell assembly.

The quadratic reflectron with 458 mm length consisting of 47 center-holed electrodes is installed such that its entrance is at the second time focus. High voltage (27 kV) applied to the 44th electrode is distributed by a voltage divider circuit to get a quadratic ($V = kx^2$) potential inside. A 98% grid is mounted on this electrode. The 45th, 46th, and 47th electrodes are kept at 26, 21, and 10 kV, respectively, with a 95% grid mounted on the 45th electrode. These are to minimize field penetration and to suppress back-transmission of ions formed by the bombardment of neutrals on various parts.

(19) Dugger, D. L.; Kiser, R. W. *J. Chem. Phys.* **1967**, *47*, 5054–5061.
(20) Haddon, W. F.; McLafferty, F. W. *Anal. Chem.* **1969**, *41*, 31–36.
(21) Cornish, T.; Cotter, R. J. *Rapid Commun. Mass Spectrom.* **1992**, *6*, 242–248.
(22) Beussman, D. J.; Vlasak, P. R.; Mclane, R. D.; Seeterlin, M. A.; Enke, C. G. *Anal. Chem.* **1995**, *67*, 3952–3957.
(23) Giannakopulos, A. E.; Thomas, B.; Colburn, A. W.; Reynolds, D. J.; Raptakis, E. N.; Makarov, A. A.; Derrick, P. J. *Rev. Sci. Instrum.* **2002**, *73*, 2115–2123.
(24) Dahl, D. A. *SIMION 3D*, version 7.0; Idaho National Labs: Idaho Falls, ID, 2000.
(25) Rockwood, A. L. *Proceedings of the 34th Annual ASMS Conference on Mass Spectrometry and Allied Topics*, Cincinnati, OH, June 8−13, 1986.

In our previous instrument,[26] the PD laser was irradiated at the first time focus. A problem was that the arrival time of a selected precursor ion pulse at this position varied a little, especially after irradiation of a sample spot over an extended period by the MALDI laser, often disturbing the ion pulse−laser pulse synchronization. In the present instrument, the PD cell is located nearly halfway between the reflectrons, viz., not at the second time focus. SIMION calculations predicted a temporally stable precursor ion pulse at this position, which was proven through actual measurements (vide infra).

Operation. Details of the methods to record MALDI-TOF (MS), postsource decay (PSD, MS^2), PD (MS^2), and voltage-on PD (MS^3) spectra are similar to those reported previously.[16−18,27,28] A nitrogen laser (VSL-337ND-S, Laser Science, Franklin, MA) is used for MALDI. Two ion gates are turned off to record MALDI-TOF spectra and turned on for MS^2 and MS^3. In PD experiments, a PD laser (193 nm, PSX-100, MPB Communication Inc., Montreal, Quebec, Canada) pulse is synchronized with the lowest mass isotopomer ("A" peak[29]) pulse of a precursor ion. A laser-off spectrum is subtracted from a laser-on spectrum to get a PD spectrum.

Samples. The peptides YPFVEPI and RLLAPITAY were purchased from Peptron (Daejeon, Korea) and the matrix, α-cyano-4-hydroxycinnamic acid (CHCA), from Sigma (St. Louis, MO). MALDI samples were prepared by the same method as described previously.[18]

Mass Calibration for Peaks in Voltage-on Spectra (MS^3). A salient feature of the quadratic reflectron[25] used in this work is that the flight time of a product ion inside the reflectron is determined only by its m/z. This results in the same flight times inside the reflectron for the in-cell, postcell, and consecutive components of m_2^+ in voltage-on PD, even though their kinetic energies are different. Both its object and image time foci are at the reflectron entrance. This is the reason why the present apparatus was designed with the second time focus at the reflectron entrance and the detector was placed immediately after the reflectron.

Velocity of the ionic species in E2−E3 is virtually the same whether dissociation has occurred or not. Hence, the high voltage applied to the PD cell only affects the flight times in E3−E4 (length l_3), in the field-free regions between E4 and the reflectron entrance (length d_1), and between the reflectron exit and the detector (length d_2). The three regions will be collectively called the "difference regions". In this work, the flight time difference between consecutive (and in-cell also) and postcell components in the difference regions will be used for mass calibration of m_i^+. It is our routine to linearly shift the time scale of a voltage-on spectrum such that the flight times of m_1^+ in the voltage-on and -off spectra coincide. Then, the postcell components can be readily identified as the peaks whose flight times are unaffected by the cell voltage.[18]

Flight Time of a Postcell Component. Let us denote the kinetic energy and velocity of m_1^+ before it enters the cell as K_0 and v_0 ($= (2K_0/m_1)^{1/2}$), respectively. As m_1^+ enters the cell floated at V, its in-cell velocity (v_I) becomes as follows.

$$v_I = v_0\{1 - (eV/K_0)\}^{1/2} \quad (1)$$

m_1^+ is accelerated between E3 and E4 (constant acceleration) and its velocity is restored to v_0 at E4. $m_1^+ \rightarrow m_2^+$ dissociation in the field-free region between E4 and the reflectron entrance forms the postcell component of m_2^+ with velocity v_0. The flight time of this component in the difference regions is as follows.

$$t_P = 2l_3/(v_0+v_I) + (d_1+d_2)/v_0 \quad (2)$$

Let us define new parameters C_1−C_3 as follows.

$$C_1 = (d_1+d_2)/(2K_0/m_1)^{1/2}, \quad C_2 = 2l_3/(d_1+d_2), \text{ and } \quad C_3 = eV/K_0 \quad (3)$$

Then, eq 2 is converted into the following form.

$$t_P = C_1[1 + C_2/\{1 + (1 - C_3)^{1/2}\}] \quad (4)$$

Flight Times of in-Cell and Consecutive Components. For a consecutive component, the ionic species at E3 is m_i^+ with the velocity v_I and the kinetic energy $(m_i/m_1)(K_0 - eV)$. m_i^+ moves with constant acceleration in E3−E4, and its kinetic energy becomes $(m_i/m_1)(K_0 - eV) + eV$ at E4. Then, its velocity (v_C^i) in the field-free region and also the velocity of m_2^+ generated from it are as follows.

$$v_C^i = \{(2K_0/m_1) + 2\,eV(m_1-m_i)/m_1m_i\}^{1/2} \quad (5)$$

The flight time for this component in the difference regions is as follows.

$$t_C^i = 2l_3/(v_I+v_C^i) + (d_1+d_2)/v_C^i = C_1\big[\{1 + C_3(m_1-m_i)/m_i\}^{-1/2} + C_2/\{(1 - C_3)^{1/2} + (1 + C_3(m_1-m_i)/m_i)^{1/2}\}\big] \quad (6)$$

Substituting $m_i = m_2$ in eq 6, the flight time for the in-cell component is obtained.

$$t_I = C_1\big[\{1 + C_3(m_1 - m_2)/m_2\}^{-1/2} + C_2/\{(1 - C_3)^{1/2} + (1 + C_3(m_1 - m_2)/m_2)^{1/2}\}\big] \quad (7)$$

Mass Calibration for m_i^+. The flight time difference between consecutive and postcell components, $\Delta t^i = t_P - t_C^i$, can be obtained from eqs 4 and 6.

$$\Delta t^i/C_1 = F^i = 1 + C_2/\{1 + (1 - C_3)^{1/2}\} - \{1 + C_3(m_1 - m_i)/m_i\}^{-1/2} - C_2/\big[(1 - C_3)^{1/2} + \{1 + C_3(m_1 - m_i)/m_i\}^{1/2}\big] \quad (8)$$

Equation 8 can be solved for m_i as follows.

$$m_i = m_1/\{1 + (X^2 - 1)/C_3\} \quad (9)$$

(26) Moon, J. H.; Yoon, S. H.; Kim, M. S. *Bull. Korean Chem. Soc.* **2005**, *26*, 763–768.
(27) Moon, J. H.; Yoon, S. H.; Kim, M. S. *Rapid Commun. Mass Spectrom.* **2005**, *19*, 3248–3252.
(28) Moon, J. H.; Yoon, S. H.; Kim, M. S. *Rapid Commun. Mass Spectrom.* **2005**, *19*, 2481–2487.
(29) McLafferty, F. W.; Turecek, F. *Interpretation of Mass Spectra*, 4th ed.; University Science Books: Sausalito, CA, 1993.

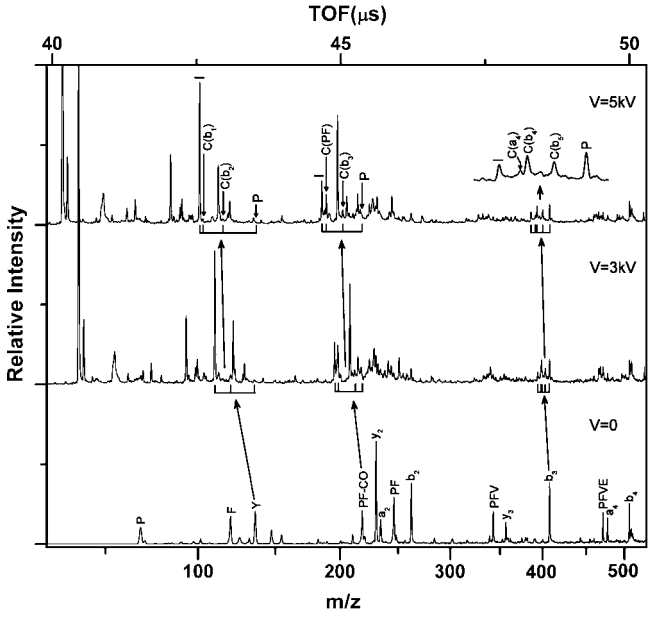

Figure 2. A 193 nm PD spectra of $[YPFVEPI + H]^+$ recorded without the cell voltage ($V = 0$) and with 3 and 5 kV on the cell. Splitting into in-cell (I), postcell (P), and consecutive (C) components is indicated by arrows for some product ions. Splitting gets larger as the cell voltage increases. m/z scale for the $V = 0$ case (regular MS^2) is shown at the bottom. The time-of-flight scale which is common to all three spectra is shown at the top.

Here, $X = [1 + C_2 - AB + \{(1 + C_2 - AB)^2 + 4AB\}^{1/2}]/2A$, $A = 1 + C_2/(1 + B) - \Delta t^i/C_1$ and $B = (1 - C_3)^{1/2}$.

RESULTS AND DISCUSSION

Mass resolving power of the instrument for MALDI-TOF (MS^1) estimated from the full widths at the half-maximum (fwhm) of peptide ion signals (not shown) measured by the final detector was around 5000. This is not as good as 10 000−13 000 achieved in our previous instruments[17,26] because optimization of the present instrument has been made mostly for voltage-on PD operation. With the instrument running under normal conditions, we also measured signals by inserting an MCP detector to the position corresponding to the center of the PD cell. Resolving power at this position was better than 2000. For ions with a m/z near 1000, fwhm at this position was around 8 ns, while ions with 1 Da different mass were separated by 20 ns. Since the pulse width of the PD laser was 5 ns, monoisotopomeric selection of the "A" peak pulse of a precursor ion could be achieved via synchronization of the laser pulse with the ion pulse. More importantly, flight times of peptide ions to this position were very stable, fluctuating by less than 0.5 ns in repeated measurements over an extended period. Hence, missing the "A" peak or hitting the "A + 1" peak by the PD laser would not occur.

The voltage-off PD spectrum for $[YPFVEPI + H]^+$ and those recorded with 3 and 5 kV on the cell are shown in Figure 2. It can be readily seen that the voltage-on spectra show far more peaks than the voltage-off spectrum due to splitting of each m_2^+ peak into components. Voltage-dependent evolution of the components of each m_2^+ can be traced by comparing the spectra recorded at various cell voltages. In particular, the postcell component of each m_2^+ can be readily identified because it remains at the same position after the coordinate shift explained

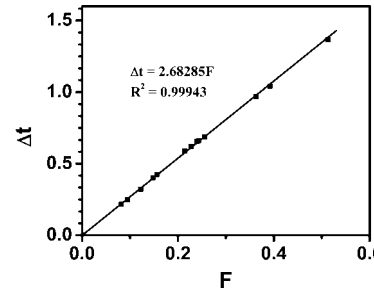

Figure 3. The Δt vs F plot for in-cell components of some selected m_2^+ in the 5 kV-on PD spectrum in Figure 2. F was calculated with $C_2 = 0.101\,23$ and $C_3 = 0.256\,41$ estimated from the design parameters and experimental high voltages. The slope in the plot was taken as the C_1 value (2.8449 μs).

previously. When m_2^+ is formed from m_1^+, the kinetics of dissociation dictates that some of it would be formed rapidly, viz., inside the cell. Then, the component of a product ion peak displaying the largest deviation from the postcell position is probably the in-cell component. As a test of this hypothesis, we calculated the m/z of such peaks in the 5 kV-on spectrum using the method explained in eqs 8 and 9 with $m_i = m_2$. Specifically, F (in eq 8) for each m_2^+ was calculated by using $C_2 = 0.101\,23$ and $C_3 = 0.256\,41$ estimated from the design parameters and high voltages used in the experiment. The Δt vs F plot in Figure 3 thus obtained was linear with a correlation coefficient of 0.9994. The slope in the plot was taken as the C_1 value (2.8449 μs), even though it was close to the estimated value. With the use of these C_1−C_3 values, the mass of each m_2^+ was calculated by eq 9. Masses thus obtained matched with correct values within a few daltons at the low- and high-mass regions. Mass errors in the intermediate mass region, 250−500 Da, were larger. The largest error was 6.6 Da observed for m_2^+ with m/z 473.2. Even though we attempted to improve the fit by slightly adjusting C_2 and C_3 values, improvement thus achieved was rather insignificant.

The mass accuracy test made above was straightforward because the mass of the in-cell component of each m_2^+ was known from the beginning. It is well-known in organic mass spectrometry[29] that loss of a neutral with 4−14 Da mass is highly unlikely. Then, ignoring H atom and H_2 molecule losses which are expected to be rare for peptide ions, the capability to reproduce product ion masses within 7 Da may be satisfactory for practical purposes. Also, the results support our assumption that the component displaying the largest deviation is the in-cell component, not a consecutive component. On the basis of the above self-consistency test, we expect that the intermediate ion masses for consecutive components can be determined within 7 Da also. In tests with other peptide ions such as $[RLLAPITAY + H]^+$, mass errors also tended to be larger for m_2^+ at intermediate masses than those at high or low masses. We suspect that mass errors are mainly due to the imperfect electric field inside the quadratic reflectron.

We used the same method and the parameters determined above to calculate the masses of consecutive components. Unless m_i^+ involved in the consecutive formation of m_2^+ is quite unstable and completely dissociates before arriving at the detector, some of it will also appear as a product ion in the voltage-off PD spectrum. Hence, we attempted to identify m_i^+ contributing to a particular consecutive component in the 5 kV-on spectrum by comparing its calculated mass with the masses of product ions in

Table 1. Mass Calibration[a] for Some Intermediate Ions (m_i^+) Forming the Final Product Ions (m_2^+) in 5 kV-On PD of $[YPFVEPI + H]^+$ (*m/z* 864.45)

m_2^+	m_i^+	correct mass	calculated mass	mass error
P	EP	227.1	224.6	−2.5
F	FV-CO	219.2	221.3	2.1
Y	b_1	164.1	162.7	−1.5
	b_2	261.1	262.7	1.6
PF-CO	PF	245.1	245.8	0.7
	b_3	408.2	409.5	1.3
y_2	y_3	358.2	361.2	3.0
	y_4	457.3	460.0	2.7
PF	PFV	344.2	348.0	3.8
b_2	b_3	408.2	410.5	2.3
	a_5	608.3	605.7	−2.6
	b_5	636.3	638.4	2.1
PFV	PFVE	473.2	477.1	3.9
	b_5	636.3	636.8	0.5
	y_6	701.4	698.7	−2.7
y_3	y_4	457.3	455.0	−2.3
	y_5	604.3	602.0	−2.3
	y_6	701.4	700.5	−0.9
b_3	a_4	479.3	477.6	−1.7
	b_4	507.3	506.9	−0.4
	b_5	636.3	632.0	−4.3
PFVE	b_5	636.3	633.8	−2.5
	y_6	702.0	699.2	−2.8
a_4	a_5+1	609.3	612.1	2.8
	b_5	636.3	635.6	−0.7
b_4	b_5	636.3	633.5	−2.8

[a] In Da.

the voltage-off spectrum. Since the main purpose of the work was to estimate the mass errors for consecutive components, weak or multiplet-looking peaks were not used. In most of the cases, we could easily correlate intermediate ions with their counterparts in the voltage-off spectrum, which allowed estimation of mass errors involved. The pattern of mass errors was qualitatively similar to that observed for the in-cell components.

On the basis of the above observation, we devised the following method to improve the mass calibration for consecutive components. From the Δt vs F data in Figure 3 for in-cell components in the 5 kV-on spectrum, we calculated the $\Delta t/F$ ratio for each m_2^+ and took it as C_1. Then, this C_1 value and previously determined C_2 and C_3 values were used to calculate the masses of the intermediate ions forming m_2^+. The results are compared with the correct intermediate ion masses in Table 1. It is to be noted that accuracy of the intermediate ion mass calibration has improved to around ±3 Da in most of the cases, the largest error being around −4 Da.

We estimated the mass resolution in MS^3 from fwhm's of consecutive components. This was around 17 Da for the $864.5^+ \rightarrow 636.3^+ \rightarrow 507.3^+$ consecutive component and 7 Da for $864.5^+ \rightarrow 227.1^+ \rightarrow 70.1^+$. Even though 17 Da resolution at the high-mass region is unsatisfactory, it may not cause much difficulty in actual analysis because there are only a few ions (m_i^+) that can generate high mass product ions (m_2^+). Quite a few consecutive pathways may contribute to the formation of a low-mass product ion. In this regard, improved mass resolution observed in the low-mass region is helpful.

In the 5 kV-on spectrum shown in Figure 2, time-of-flight positions of the in-cell components deviated substantially from those of the corresponding postcell components. This resulted in intermixing of the in-cell, consecutive, and postcell components from neighboring product ions (m_2^+), especially in the low-mass region. Components contributing to each m_2^+ clustered better at the 3 kV cell voltage. Use of a longer reflectron or lower high voltage on it, which increases the flight time of each m_2^+, would further improve clustering of the components belonging to the same m_2^+.

As has been mentioned in the introductory section, the drastic loss in sensitivity is one of the main difficulties in sequential MS^n. In contrast, fully multiplexed detection made in this work resulted in good sensitivity for MS^3 spectra. Another reason for good sensitivity is that an m_2^+ signal in the PD spectrum is partitioned into a small number of consecutive components. With regard to sensitivity, we attempted to estimate the reflection efficiency of precursor and product ions by the quadratic reflectron, which was 100% in SIMION calculations. For precursor ions, adding this reflectron resulted in roughly a 30% reduction of intensity. Measurement was difficult for product ions. The reflection efficiencies for product and precursor ions may be similar because the total product ion intensity is comparable to the precursor ion depletion by PD.

It is to be pointed out that PD is not the prerequisite for the fully multiplexed MS^3 reported in this work. The same may be achieved with CAD by floating the collision cell at high voltage. A requirement to get high quality CAD-MS^3 spectra would be good differential pumping such that collisional activation occurs mostly inside the cell. Using a pulsed valve[30] may be an alternative. By modification of the instrumentation presented in this paper, it may be possible to extend the present technique to MS^4 or even further. Adding another voltage-floated cell(s) with or without collision gas may achieve it.

CONCLUSION

Even though the possibility to construct a fully multiplexed tandem TOF for MS^3 was indicated in our previous work, difficulty in mass assignment was the major obstacle. This difficulty has been more or less removed in the new instrument reported in this work which incorporates a quadratic reflectron. The design idea reported here may be used to convert existing tandem TOF instruments into multiplexed MS^3. Also, MS^n TOF can be an inexpensive commercial alternative to FT-MS. The present instrument would be useful for the mechanistic study of peptide ion dissociation. Analytically, the method used in the present instrumentation may find application to highly selective identification of components in complex mixtures. An intriguing aspect of the present method is the possibility to detect an intermediate ion, indirectly in the form of its dissociation products, as far as its lifetime is longer than 100 ns. This presents an exciting new possibility of finding short-lived ionic species. Development of new analytical methods based on transient ion detection may follow.

ACKNOWLEDGMENT

This work was financially supported by the Korea Research Foundation, Republic of Korea, and by the Biosignal Analysis Technology Innovation program (Grant M10645010002-06N4501-00210) of the Ministry of Education and Science, Republic of Korea. Y. S. Shin thanks the Ministry of Education and Science, Republic of Korea, for Brain Korea 21 Fellowship.

Received for review August 9, 2008. Accepted October 14, 2008.

AC801675R

(30) Cornish, T. J.; Cotter, R. J. *Anal. Chem.* **1993**, *65*, 1043–1047.